SIANI
INSTITUTO UNIVERSITARIO
INGENIERIA COMPUTACIONAL

18th Spanish-French School Jacques-Louis Lions about Numerical Simulation in Physics and Engineering

Solar radiation modeling and forecasting

F. Díaz, G. Montero, R. Montenegro, L. Mazorra, E. Rodríguez, J.M. Escobar

Las Palmas de Gran Canaria, 25-29 June 2018

UNIVERSIDAD DE LAS PALMAS
DE GRAN CANARIA

Solar Radiation Modeling

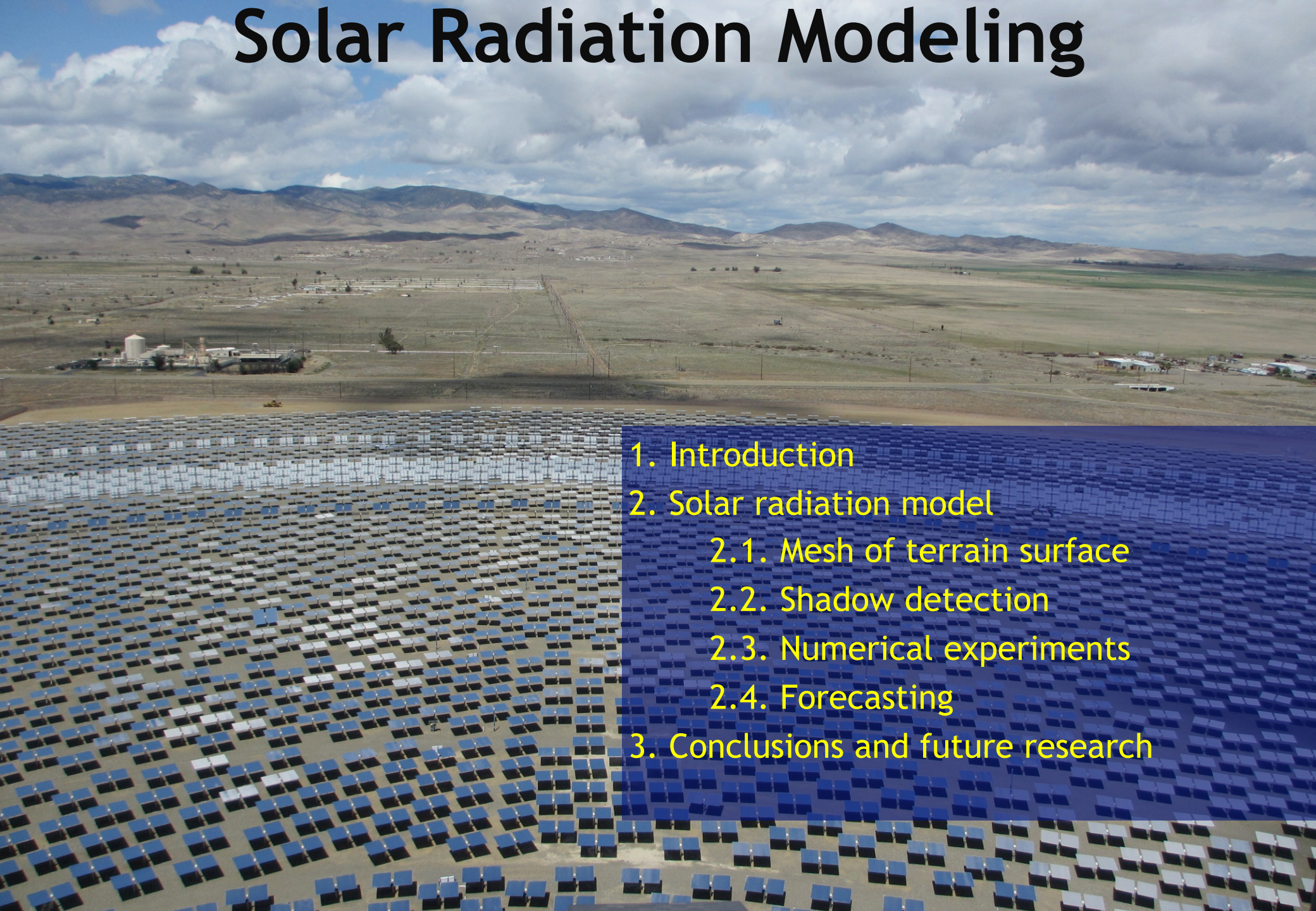

1. Introduction
2. Solar radiation model
    - 2.1. Mesh of terrain surface
    - 2.2. Shadow detection
    - 2.3. Numerical experiments
    - 2.4. Forecasting
3. Conclusions and future research

Solar radiation modeling
Introduction

SIANI

- Solar power is one of the most appreciate renewable energies in the world

- Three groups of factors determine the interaction of solar radiation with the earth's atmosphere and surface

a. The Earth's geometry, revolution and rotation (declination, latitude, solar hour angle)

b. Terrain (elevation, albedo, surface inclination/orientation, shadows)

c. Atmospheric attenuation (scattering, absorption) by

  c.1. Gases (air molecules, ozone, CO_2 and O_2)

  c.2. Solid and liquid particles (aerosols, including non-condensed water)

  c.3. Clouds (condensed water)

- We focus the study on the accurate definition of the terrain surface and the produced shadows by using an adaptive mesh of triangles

Solar radiation modeling
Introduction

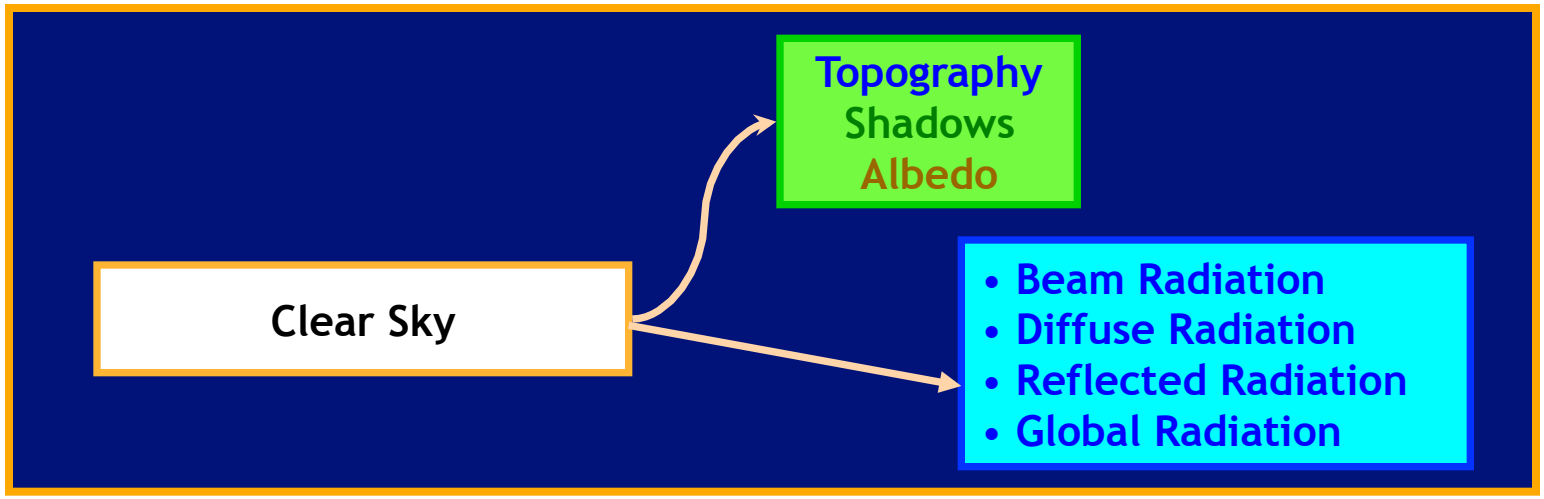

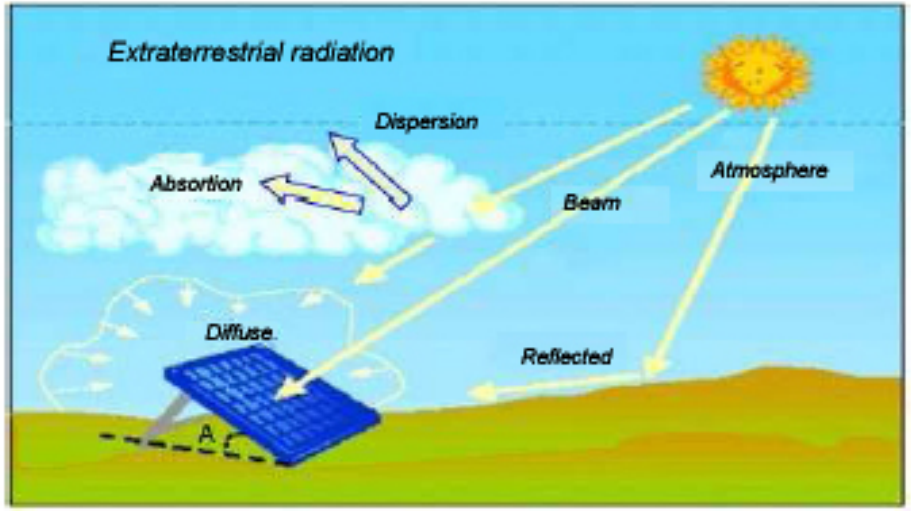

Solar radiation modeling
Introduction

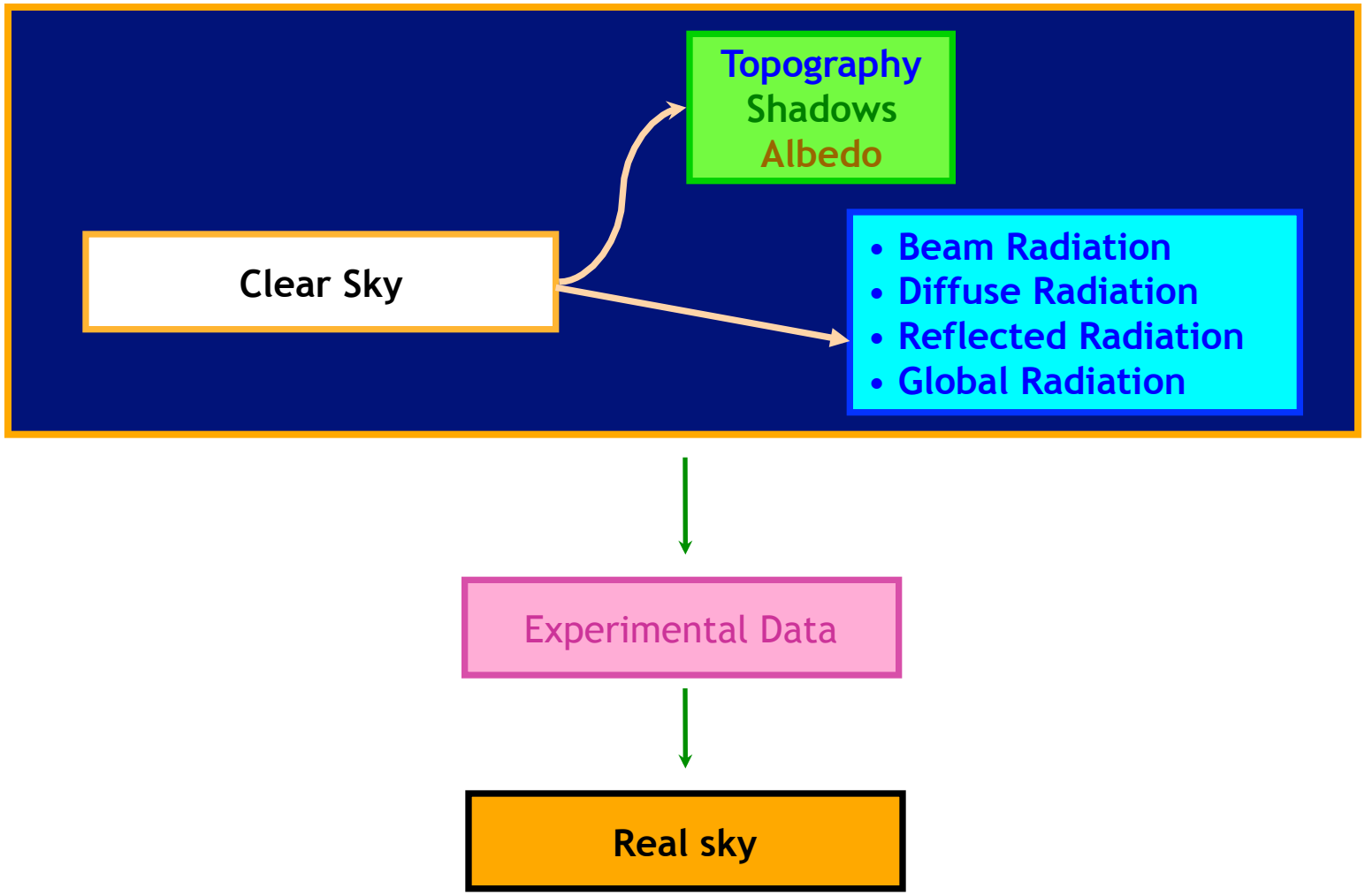

Solar radiation modeling

Terrain surface mesh

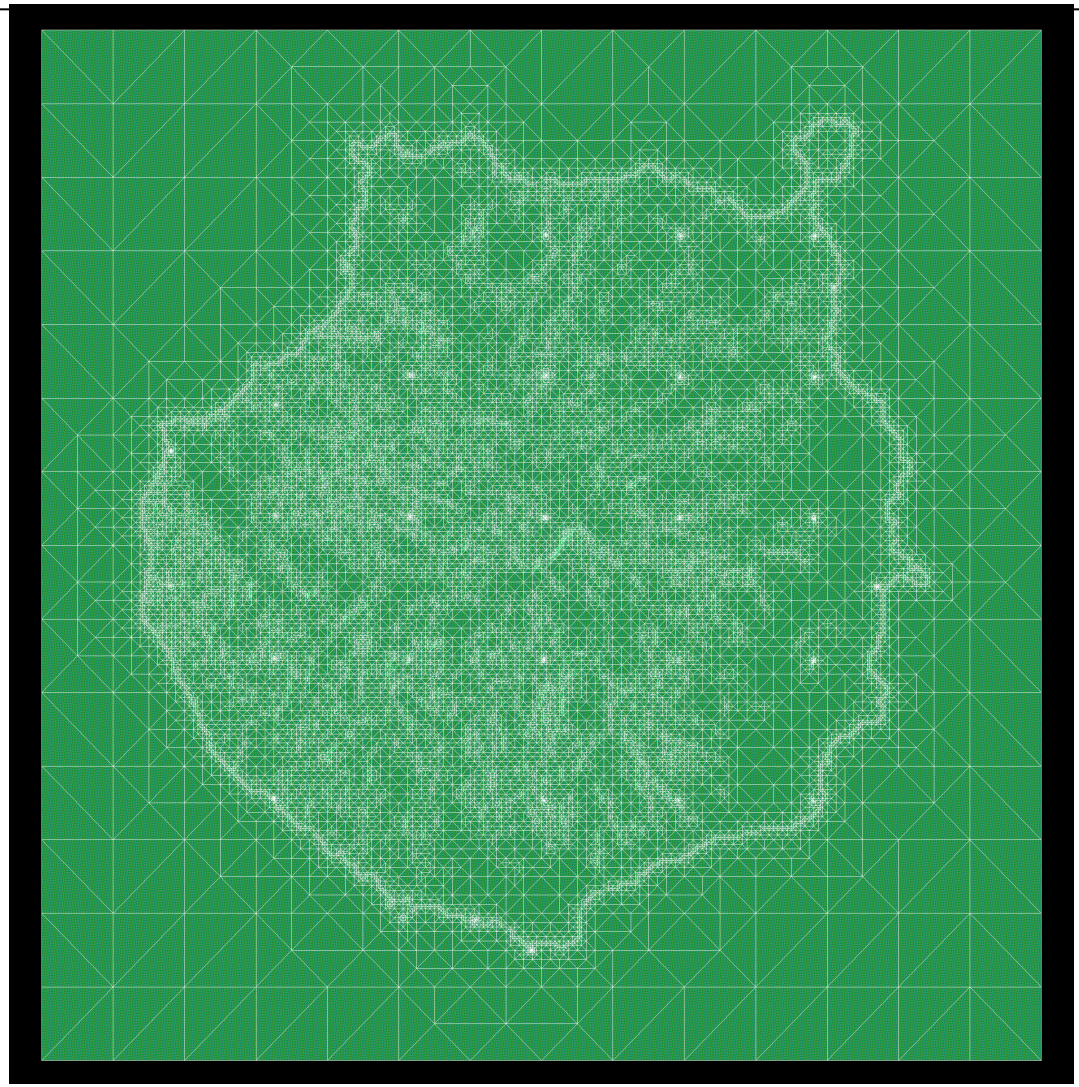

Solar radiation modeling
Terrain surface mesh

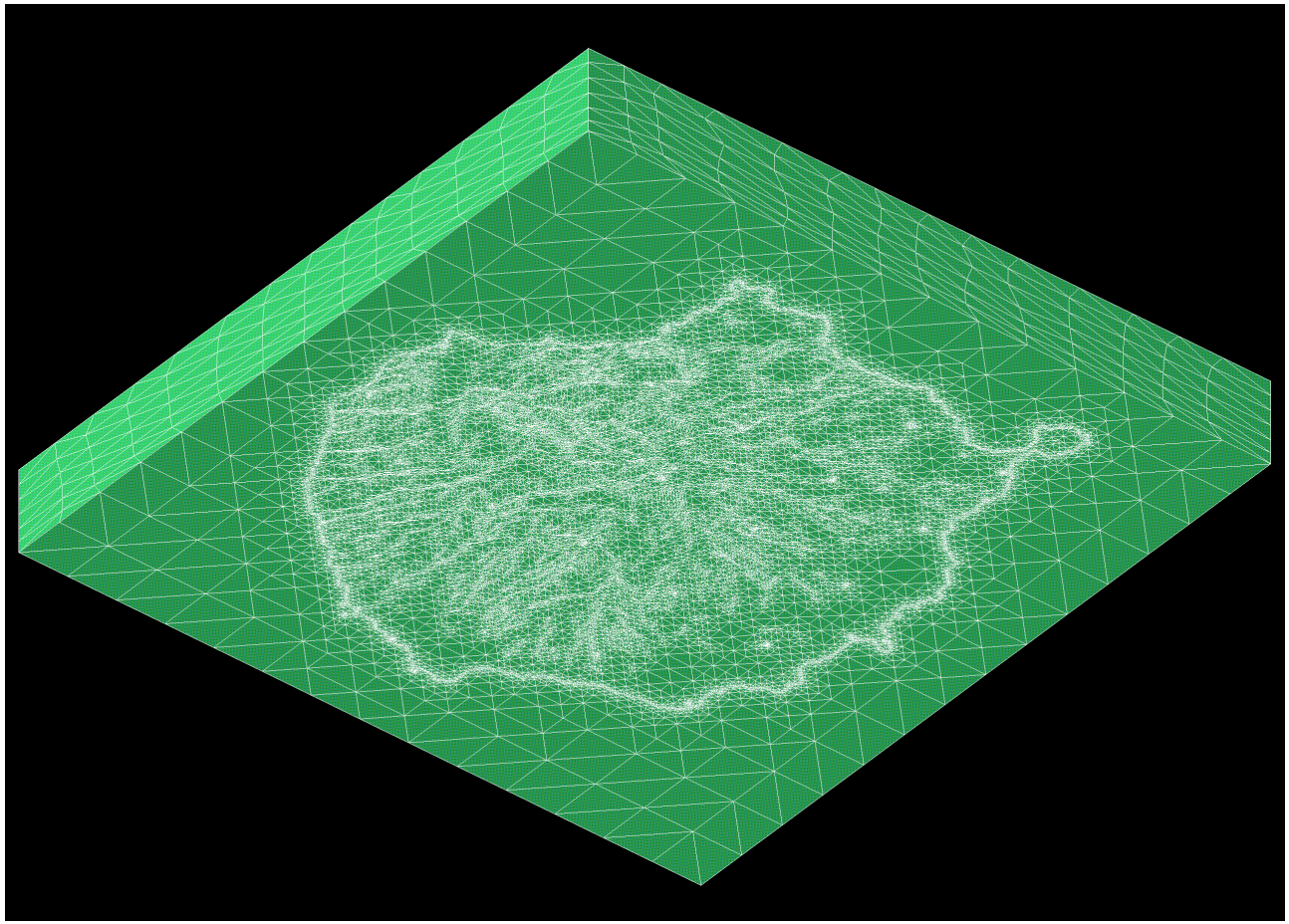

Solar radiation modeling

Terrain surface mesh

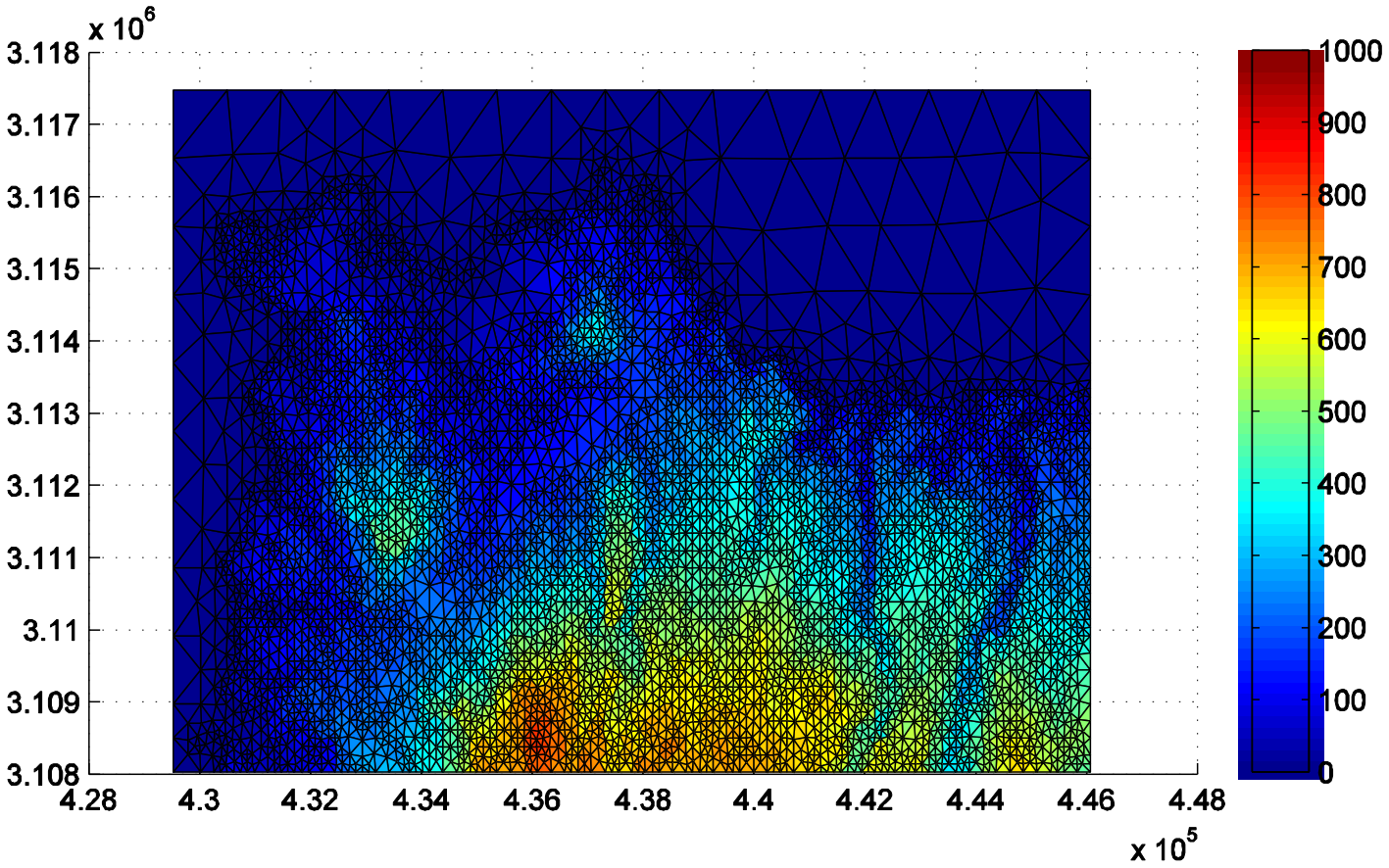

Solar radiation modeling
Shadow detection

Accurate evaluation of radiation

Shadow detection

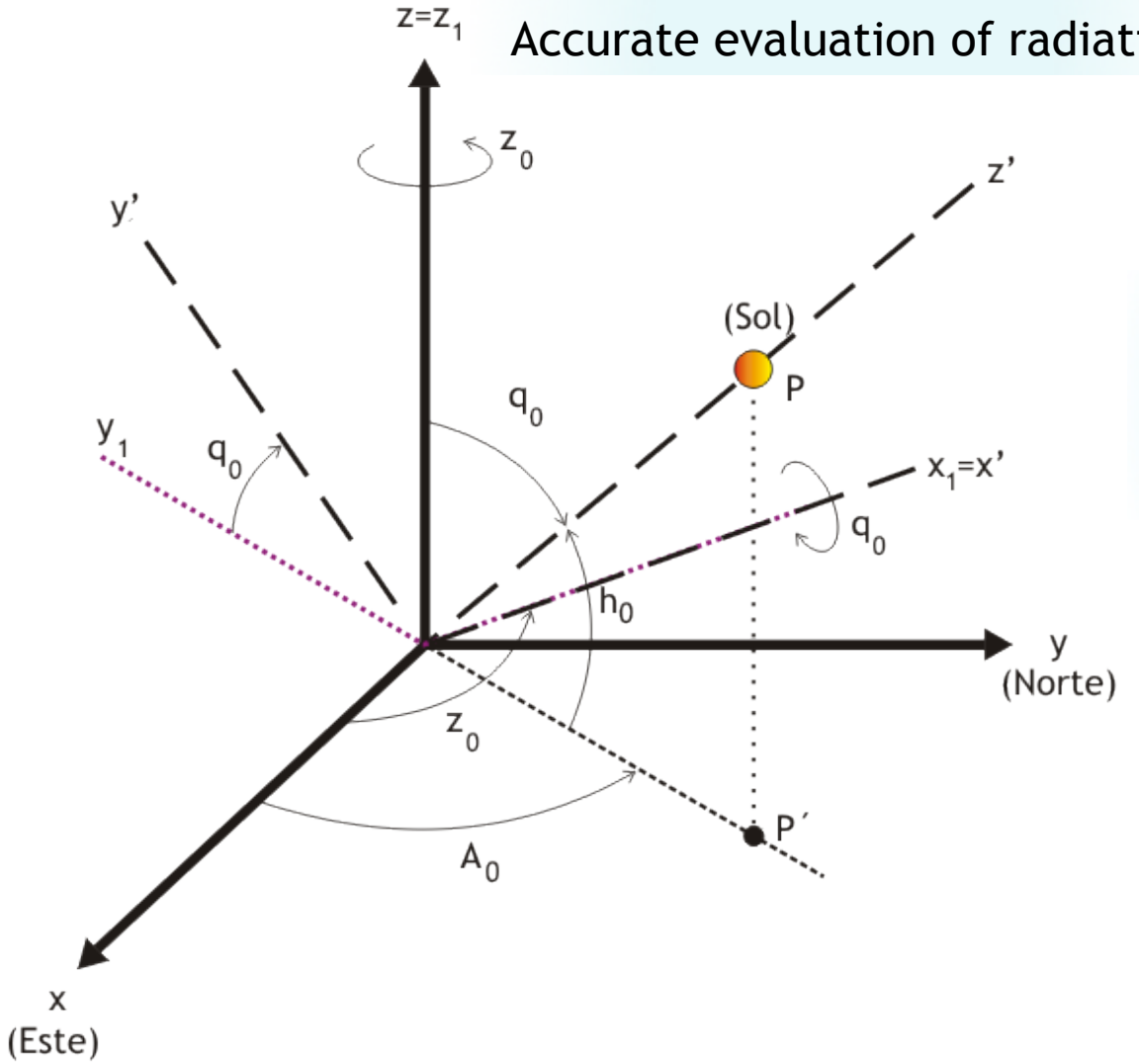

Construct a reference system *x'*, *y'* and *z'*, with *z'* in the direction of the beam radiation. Mesh is projected on the plane *x'y'*

Solar radiation modeling
Shadow detection

Incidence angle (δ_{exp})

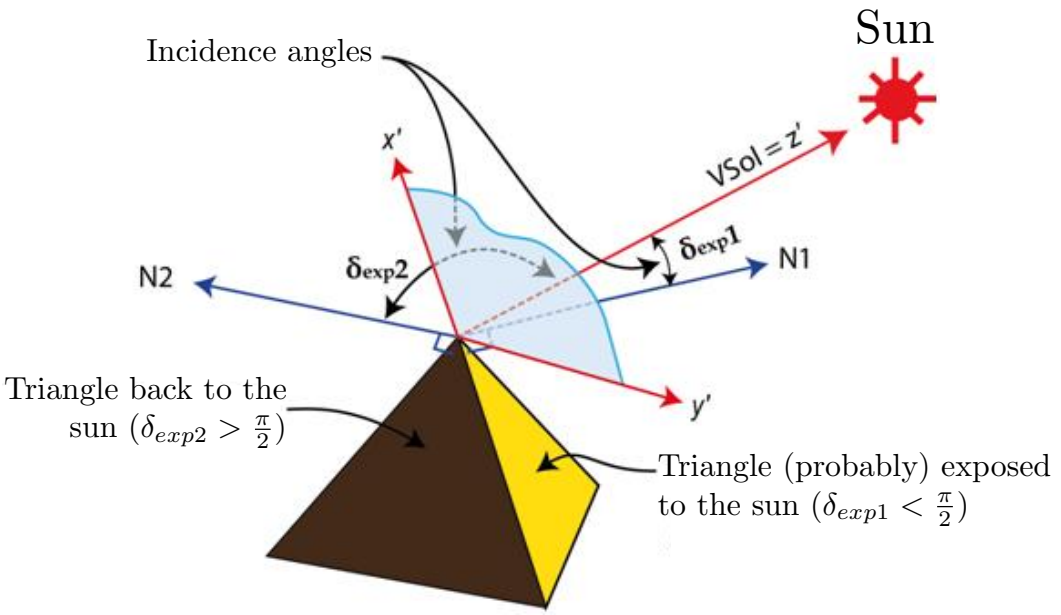

Own shadows

$$L_{fss} = \begin{cases} 0 & \text{if } (|\delta_{exp}| \geq (\pi/2)) \\ 1 & \text{if } ((\pi/2) > |\delta_{exp}| \geq 0) \end{cases}$$

Solar radiation modeling
Shadow detection

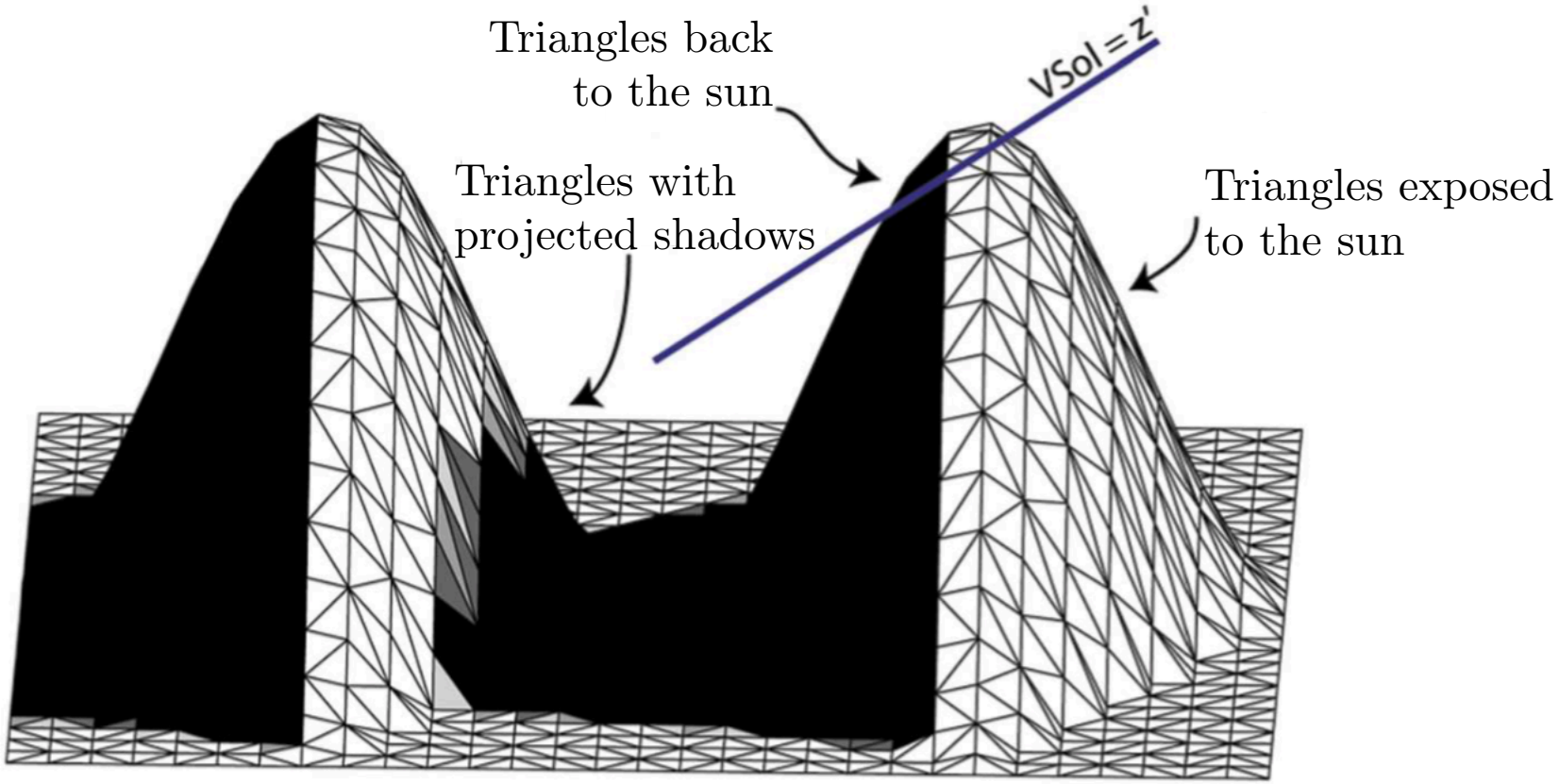

Solar radiation modeling
Shadow detection

Projected shadows

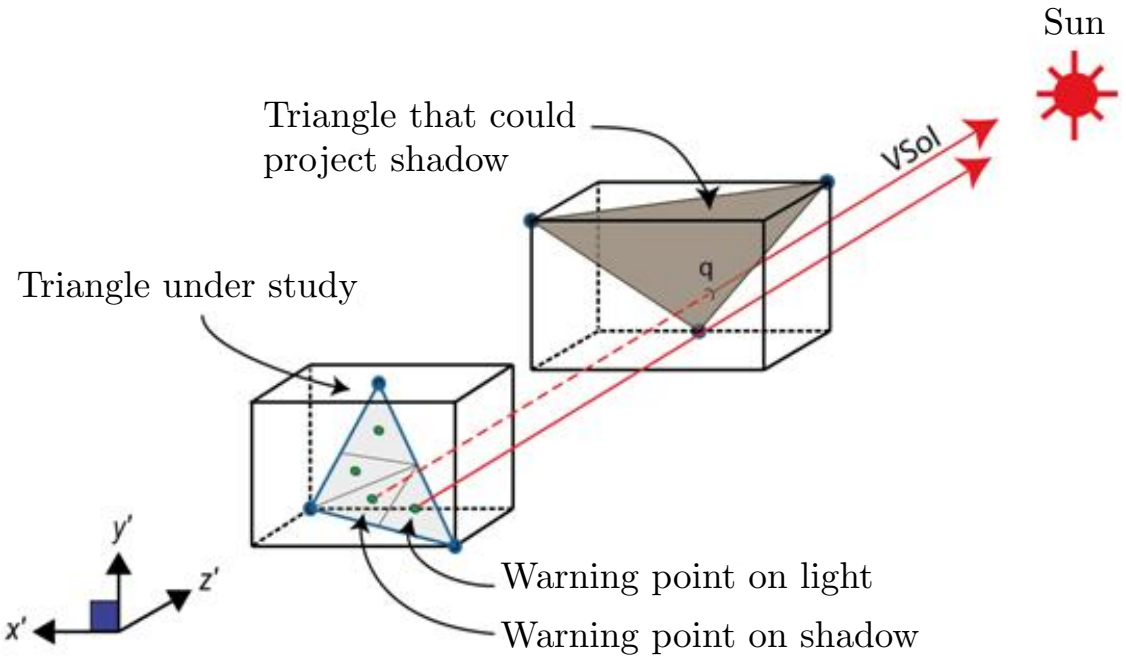

Warning Points

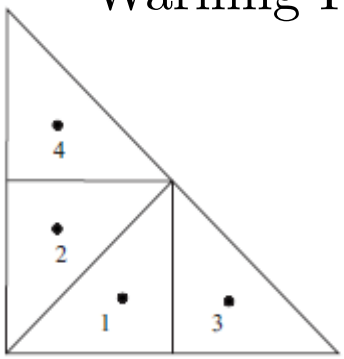

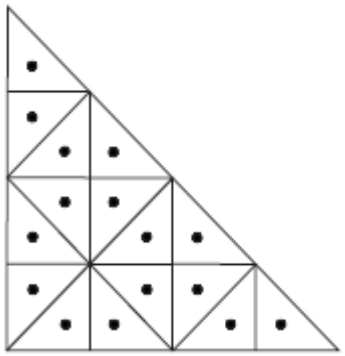

$$L_{fcs} = \frac{n_{wp} - i}{n_{wp}}$$

$$i = 0, 1, \ldots, n_{wp}$$

$$L_f = L_{fcs} \cdot L_{fss}$$

Solar radiation modeling
Shadow detection

12:00

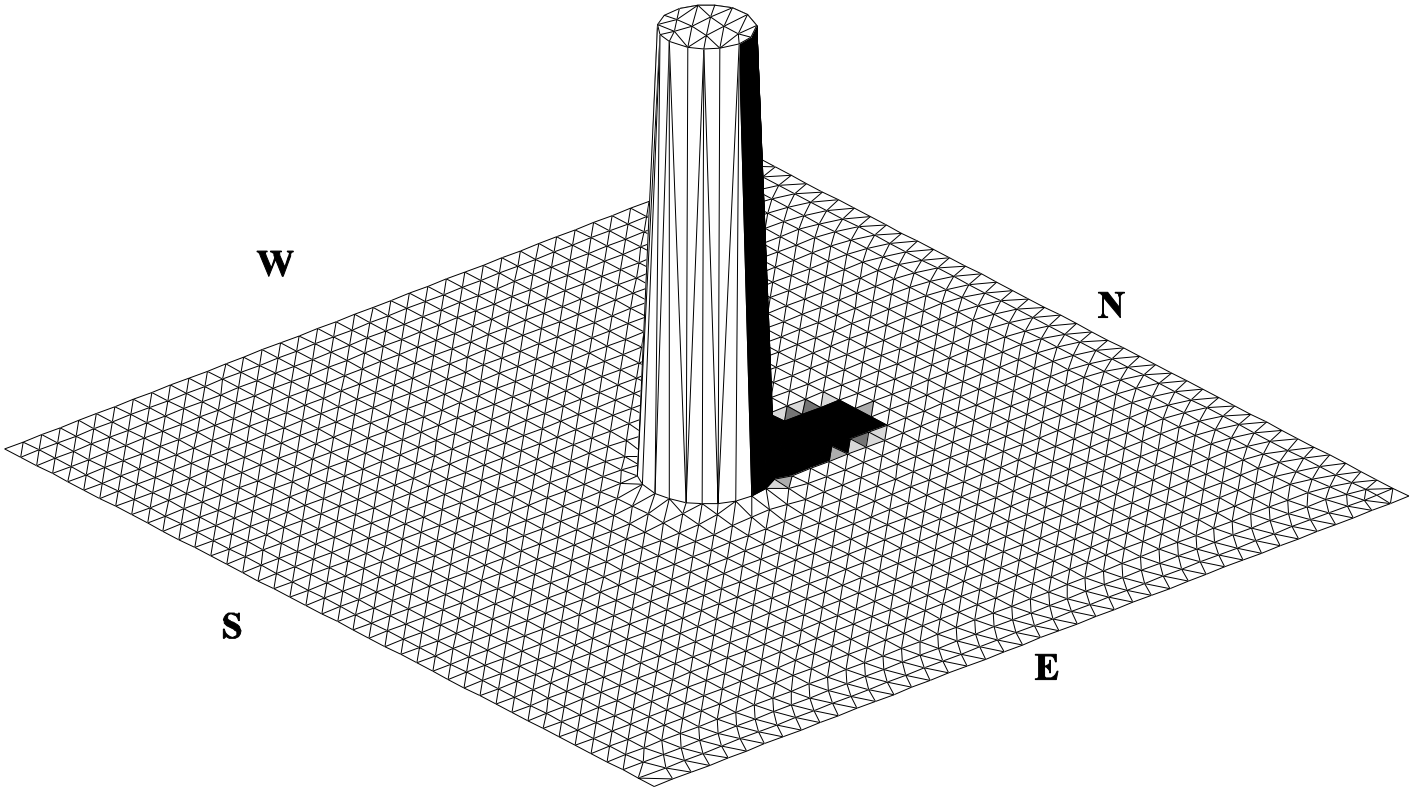

Solar radiation modeling
Shadow detection

14:00

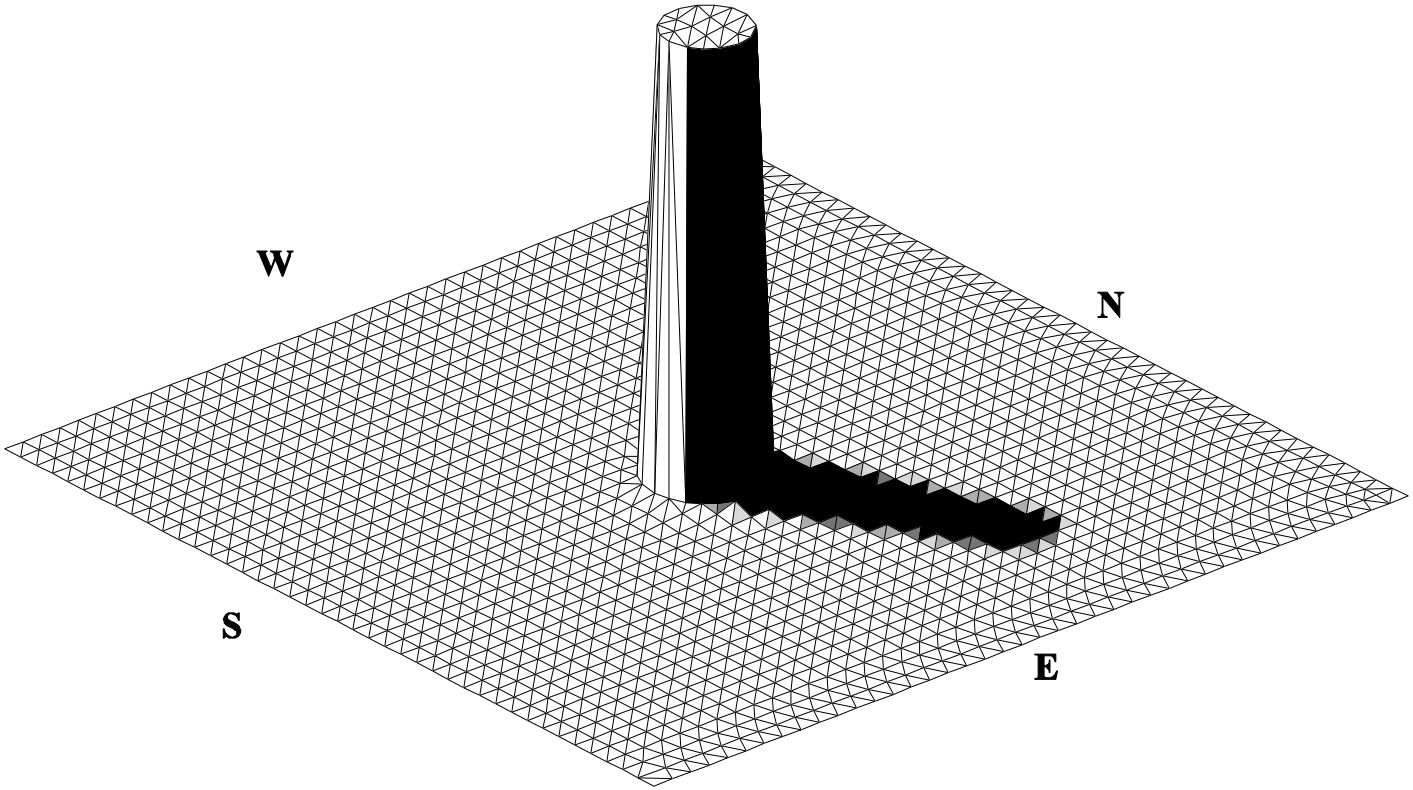

Solar radiation modeling
Shadow detection

16:00

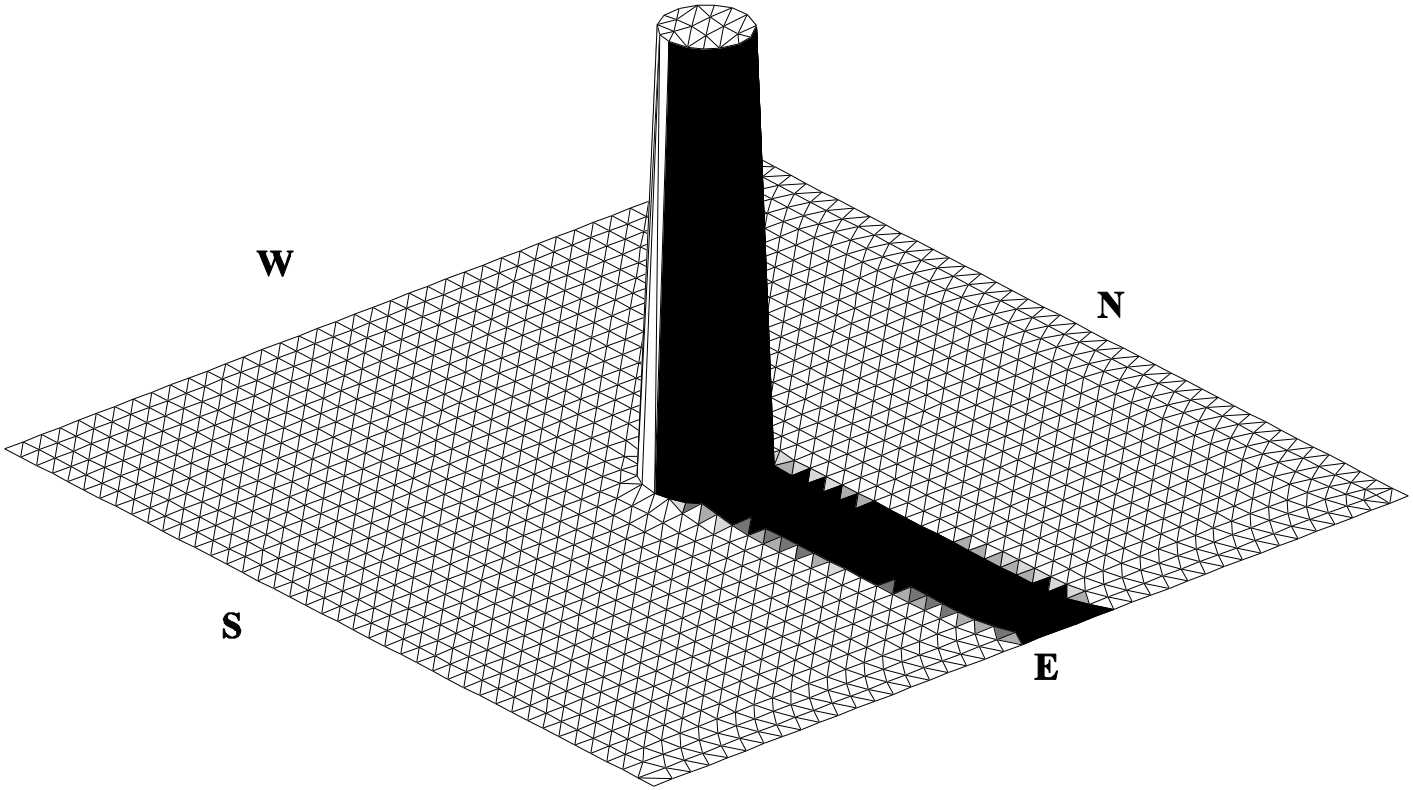

Solar radiation modeling
Shadow detection

18:00

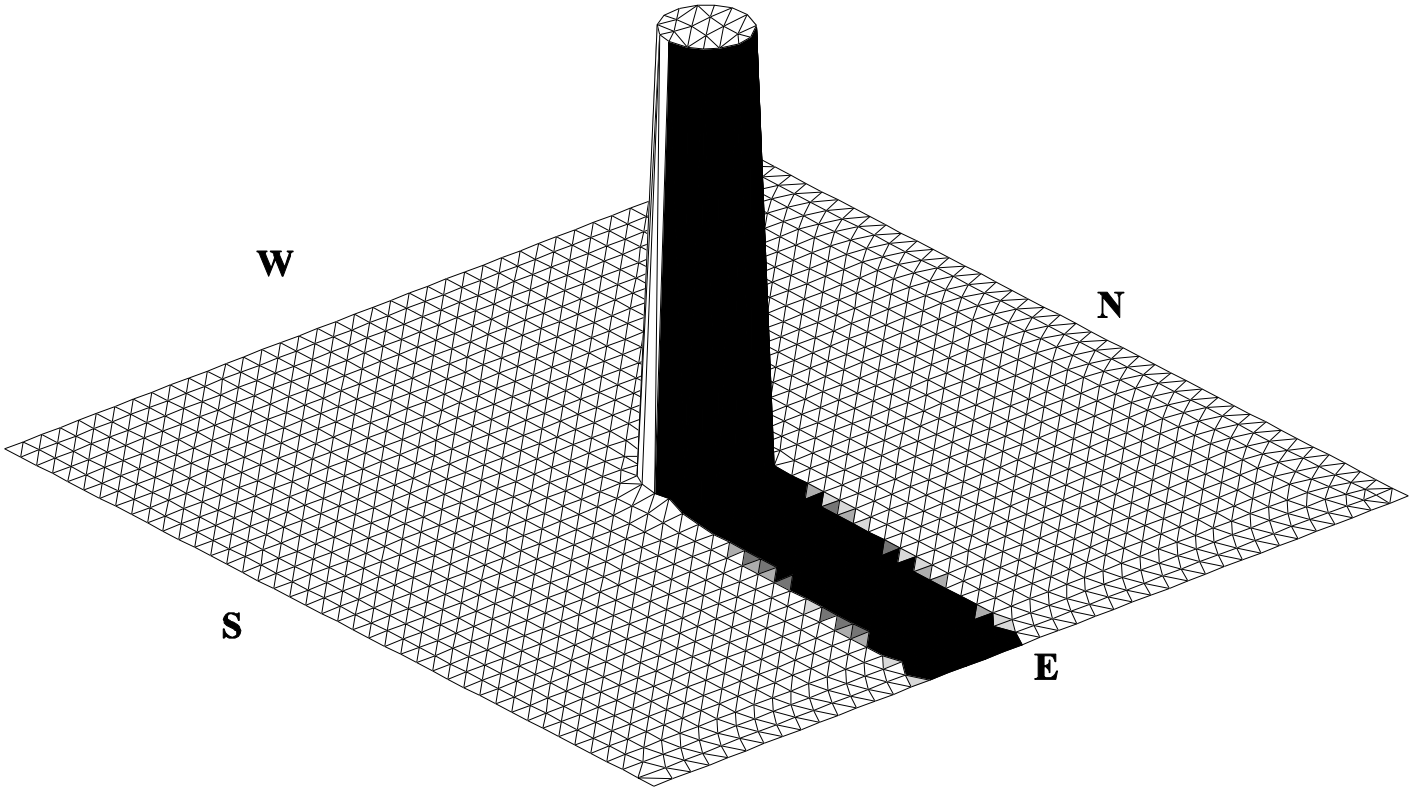

Solar radiation modeling
Shadow detection

12:00

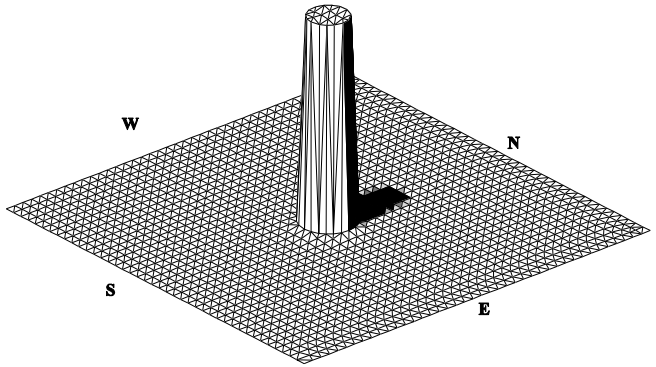

14:00

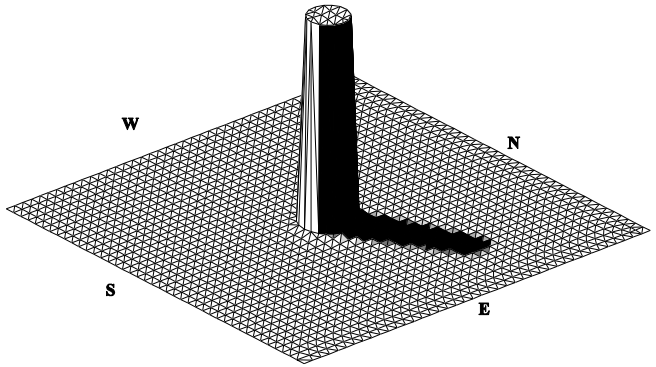

16:00

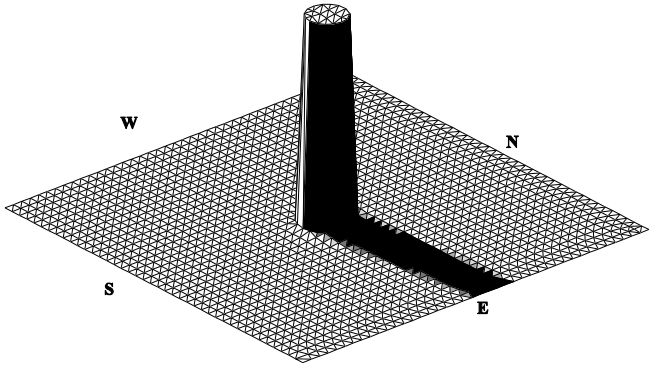

18:00

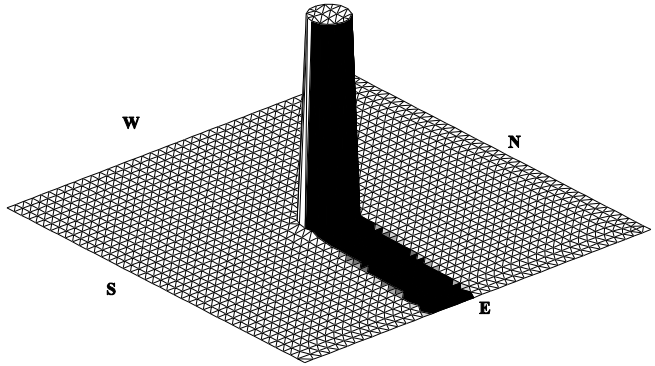

Solar radiation modeling

Solar radiation model. Solar radiation under overcast sky

The values of global irradiation on a horizontal surface for real sky (overcast) conditions *G(0)* are calculated as a correction of those of clear sky $G_c(0)$ with the clear sky index k_c

$$G(0) = G_c(0) k_c$$

If some measures of global radiation G_s are available at different measurement stations, s, the value of the clear sky index at those points may be computed as

$$k_{cs} = \frac{G_s(0)}{G_c(0)}$$

Then k_c may be interpolated in the whole studied domain, using, for example:

$$k_c = \varepsilon \frac{\sum_{n=1}^{N} \frac{k_{cn}}{d_n^2}}{\sum_{n=1}^{N} \frac{1}{d_n^2}} + (1 - \varepsilon) \frac{\sum_{n=1}^{N} \frac{k_{cn}}{|\Delta h_n|}}{\sum_{n=1}^{N} \frac{1}{|\Delta h_n|}}$$

Solar radiation modeling
Numerical experiments

Geolocation of different sites on Gran Canaria Island. Beside latitude, longitude and height (m) of each station place, the corresponding description of village is provided.

Island	Site	Latitude	Longitude	Height
Pozo Izquierdo	C0	27.8175 N	15.4244 W	47
Las Palmas de G. C.	C1	28.1108 N	15.4169 W	17
La Aldea de San Nicolás	C2	27.9901 N	15.7907 W	197
San Fernando de M.	C4	27.7716 N	15.5841 W	265
Santa Brígida	C5	28.0337 N	15.4991 W	525
Mogán (village)	C6	27.8839 N	15.7216 W	300
Sardina de Gáldar	C7	28.1681 N	15.6865 W	40
Airport	AP	27.9325 N	15.3897 W	26
Maspalomas	MP	27.7500 N	15.5667 W	25

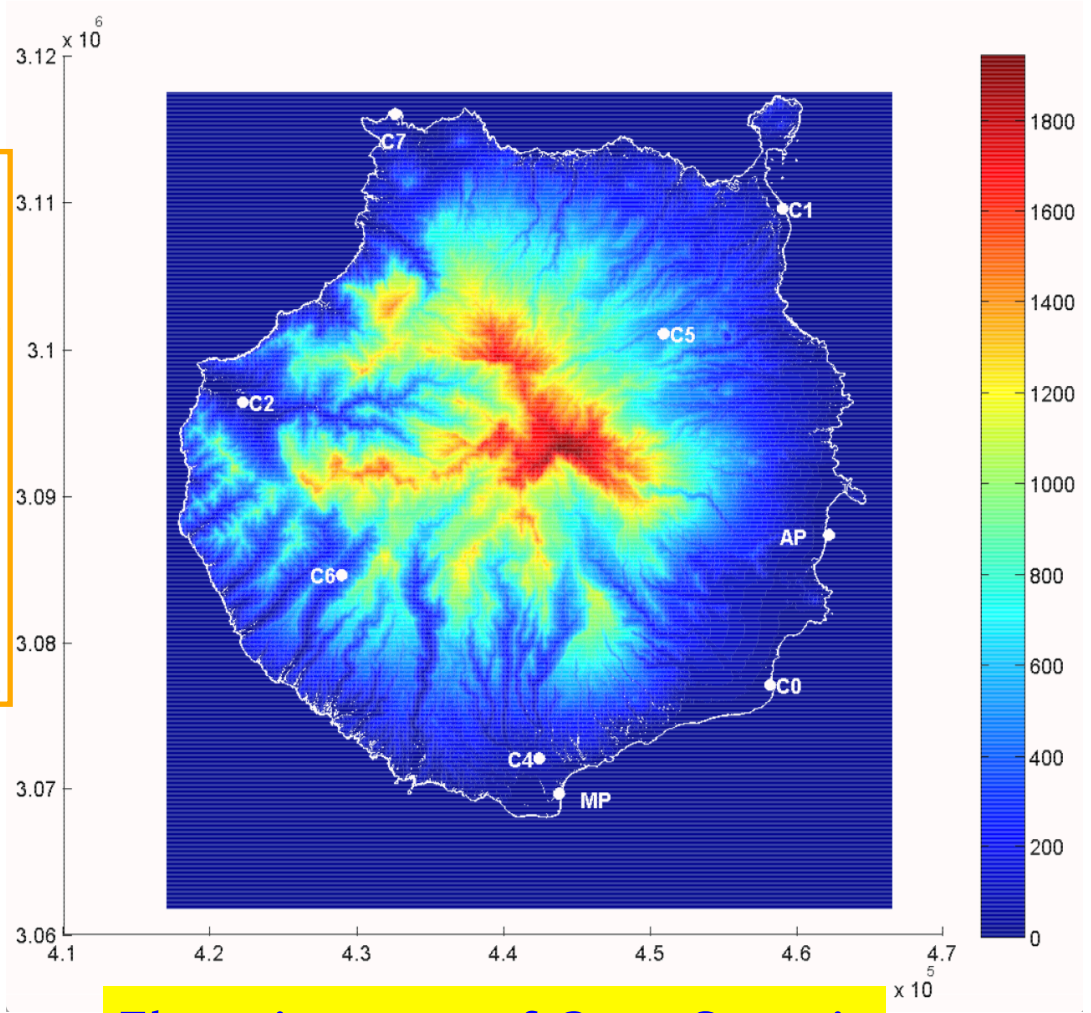

Elevation map of Gran Canaria

Solar radiation modeling
Numerical experiments

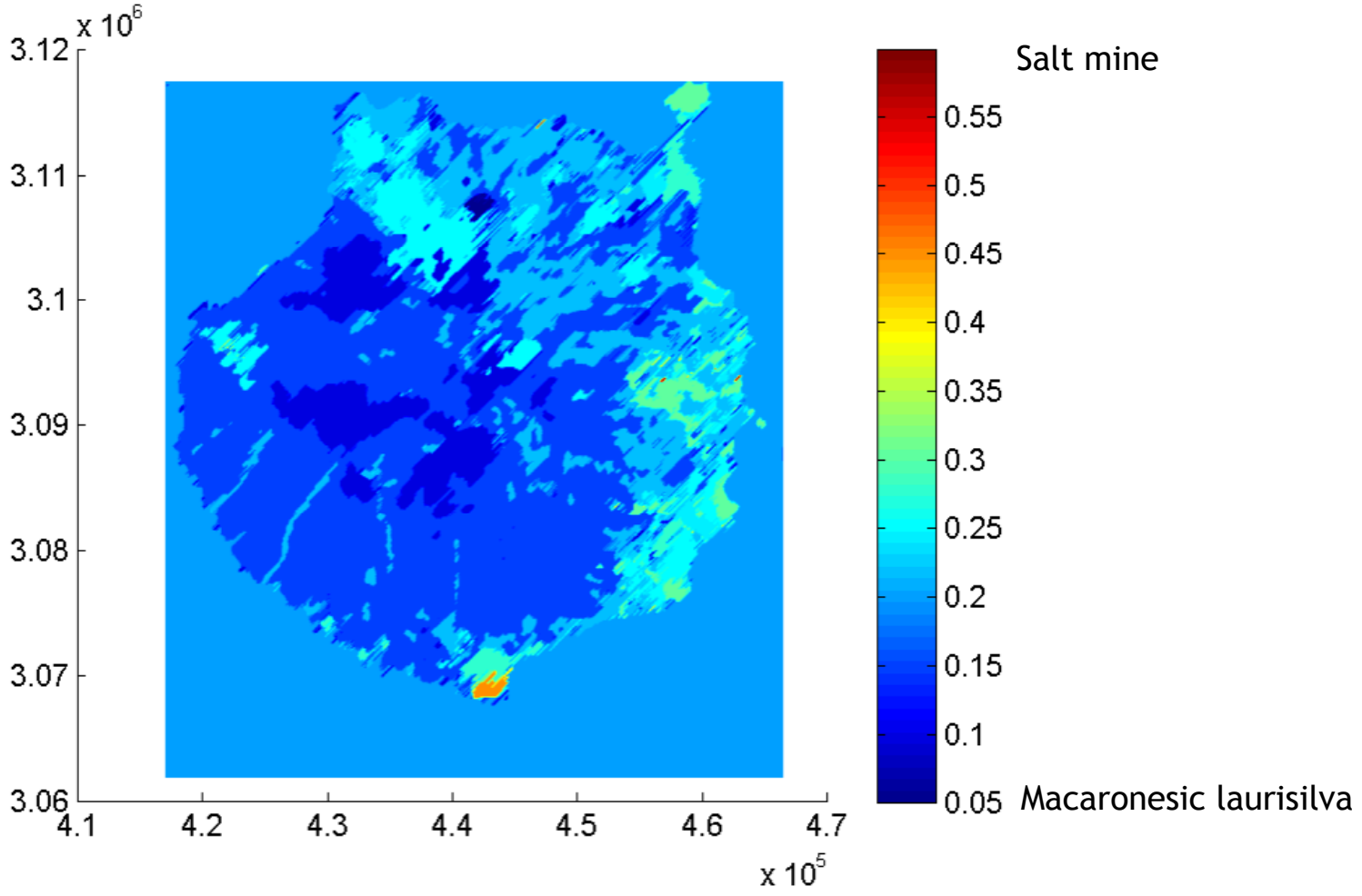

Albedo map of Gran Canaria

Solar radiation modeling

Numerical experiments

Radiation maps (J/m^2) - October 2006

82 – 83% of the mean global irradiation

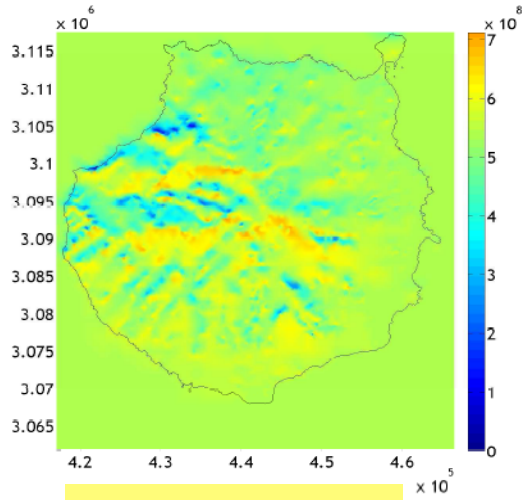

Beam radiation

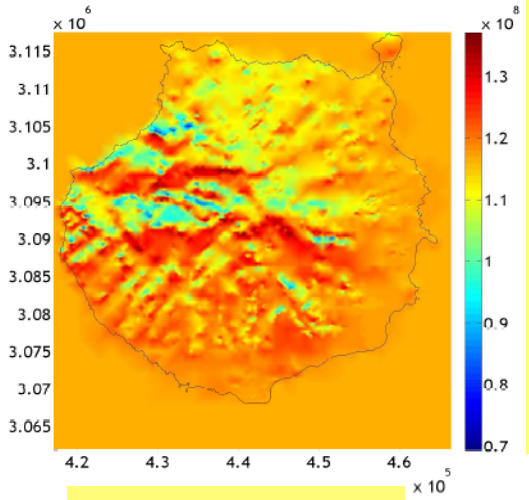

Diffuse radiation

16 – 17% of the mean global irradiation

0 – 0.4% of the mean global irradiation

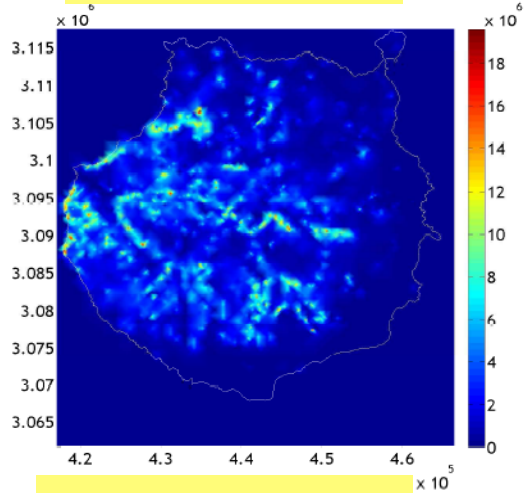

Reflected radiation

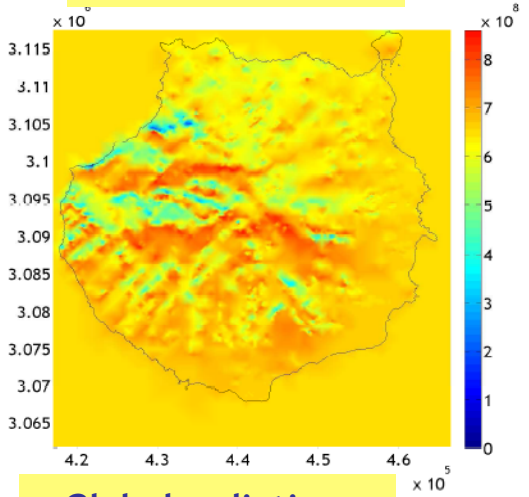

Global radiation

Solar radiation modeling
Numerical experiments

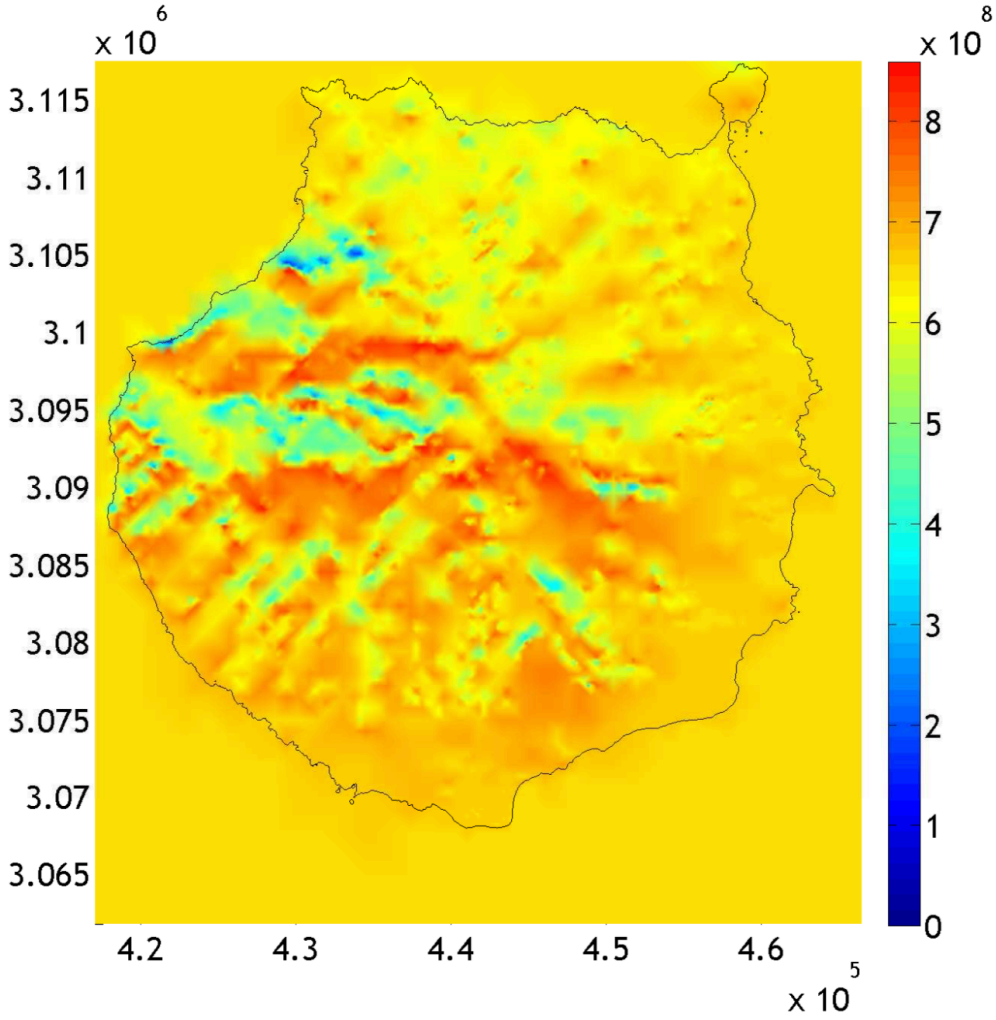

Global clear sky radiation map (J/m2)
October 2006

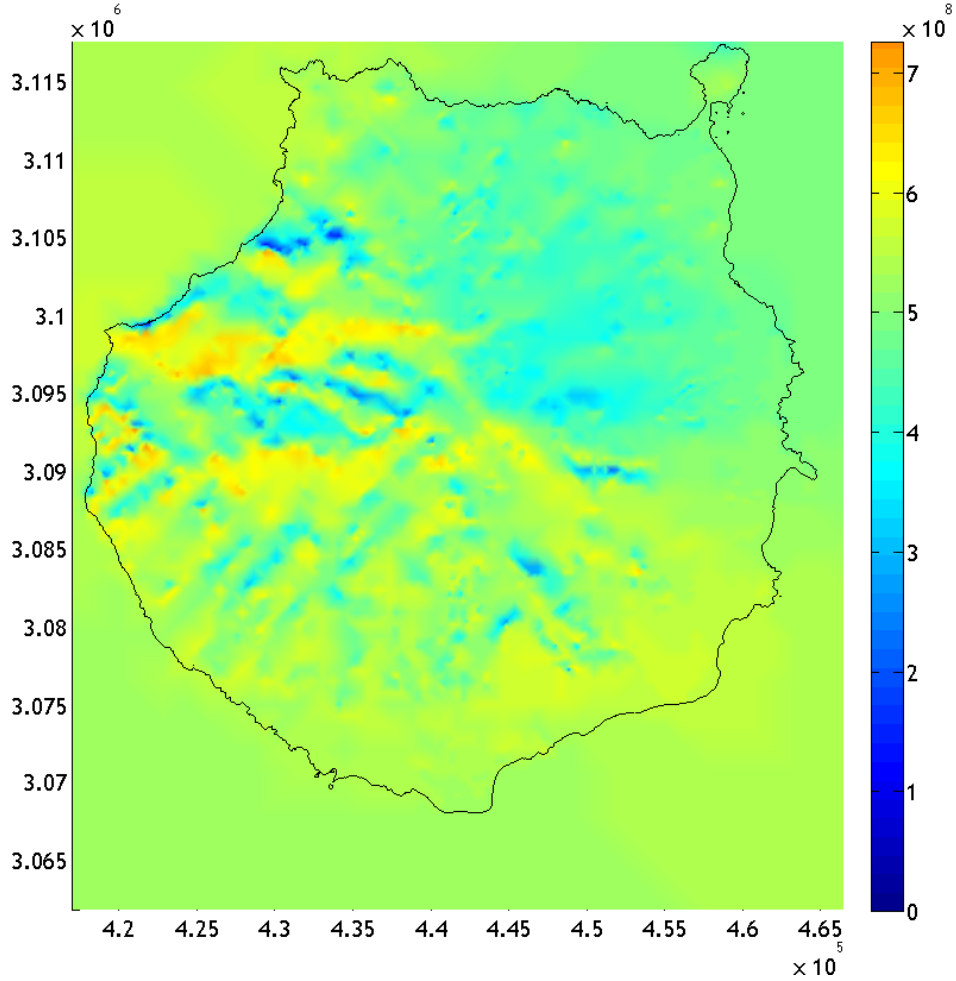

Overcast global radiation map (J/m2)
October 2006

Solar radiation modeling
Numerical experiments

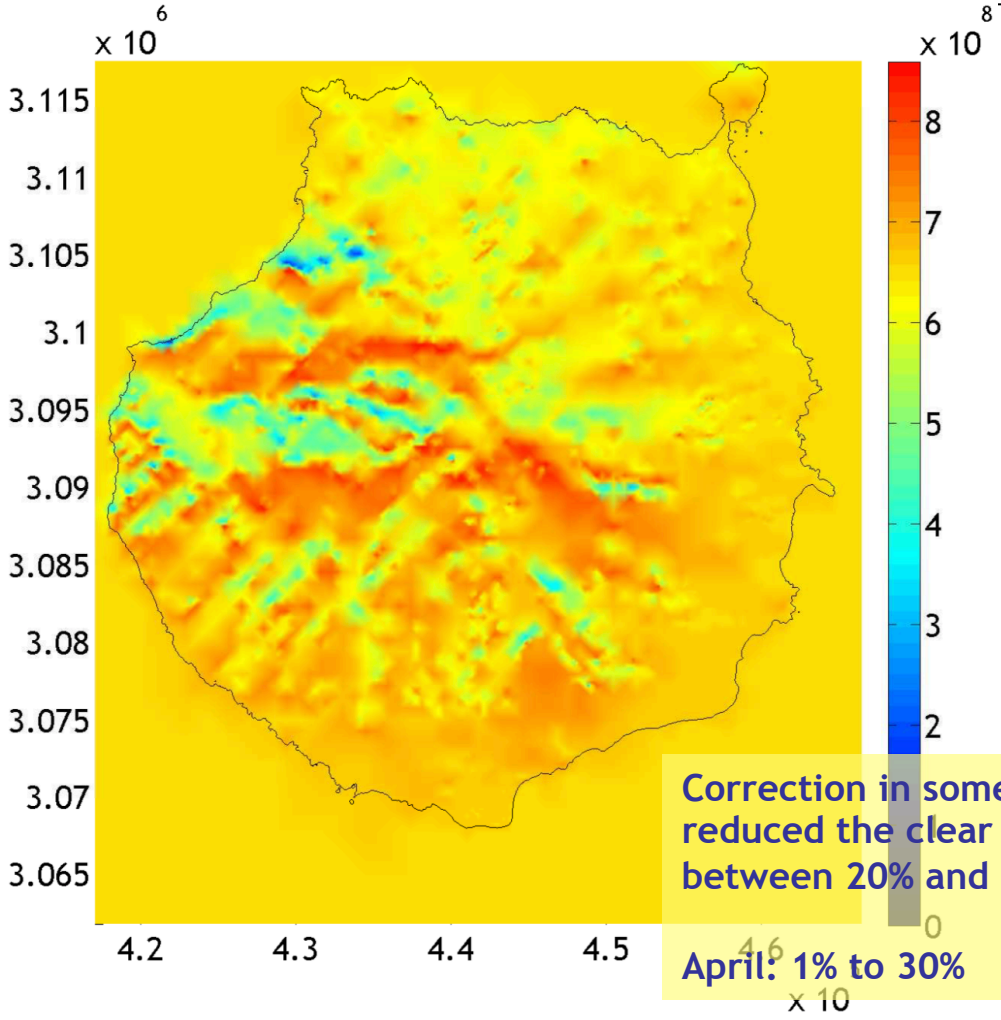

Global clear sky radiation map (J/m2)
October 2006

Correction in some overcast days reduced the clear sky results between 20% and 70% (winter)

April: 1% to 30%

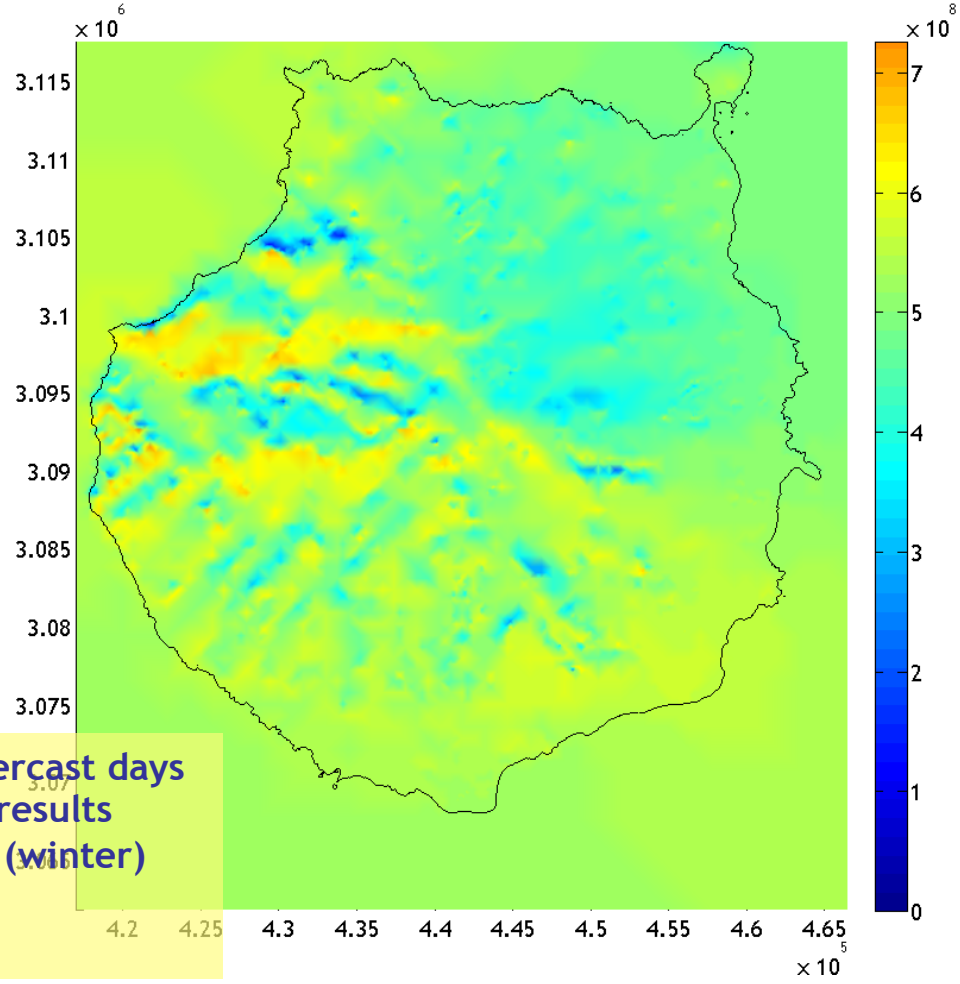

Overcast global radiation map (J/m2)
October 2006

Solar radiation modeling
Numerical experiments

SIANI

Trade wind (NE) - Alisios

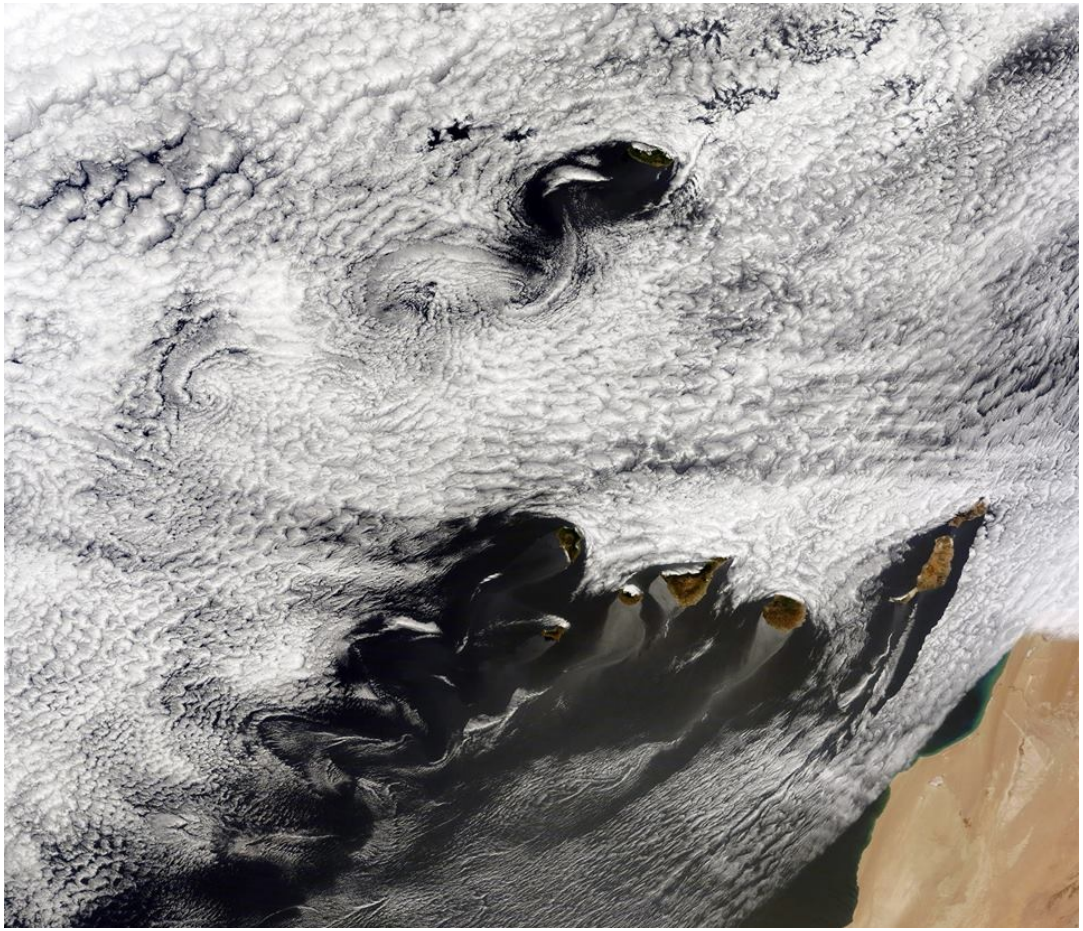

Solar radiation modeling
Numerical experiments

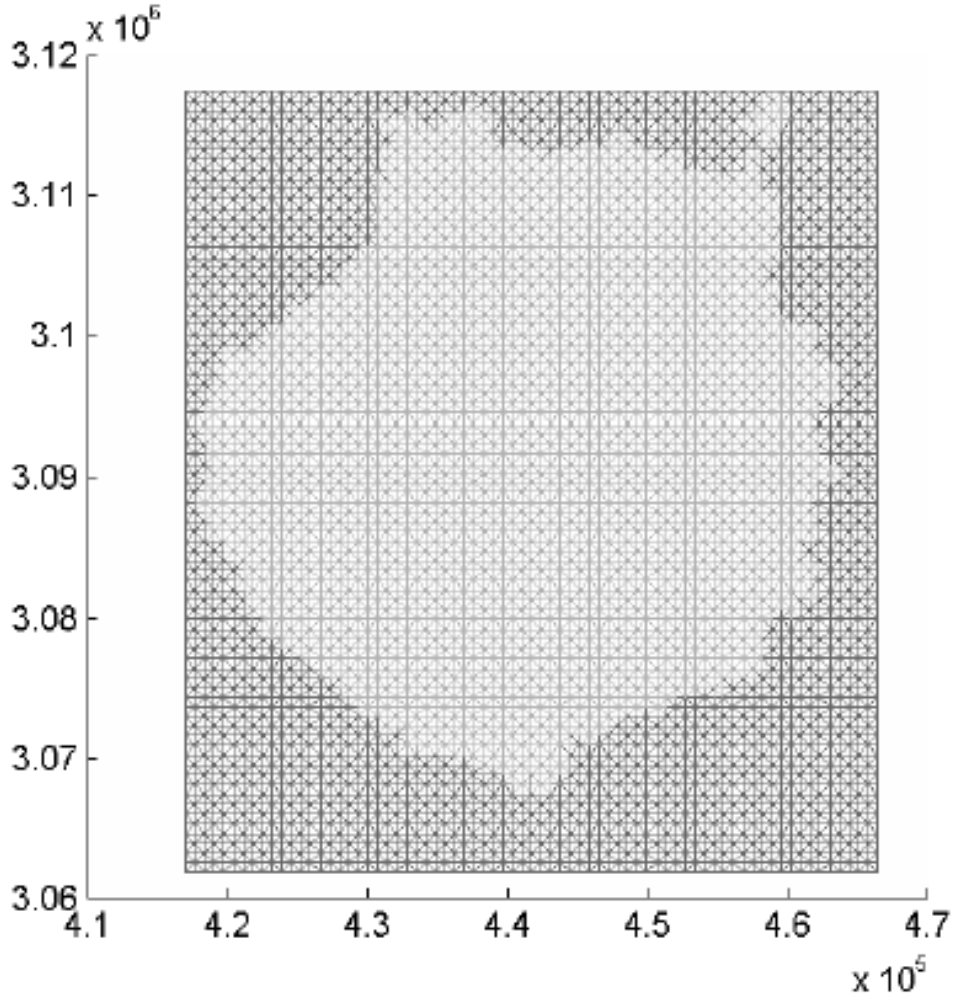

Regular mesh
5913 nodes
11520 triangles

Solar radiation modeling
Numerical experiments

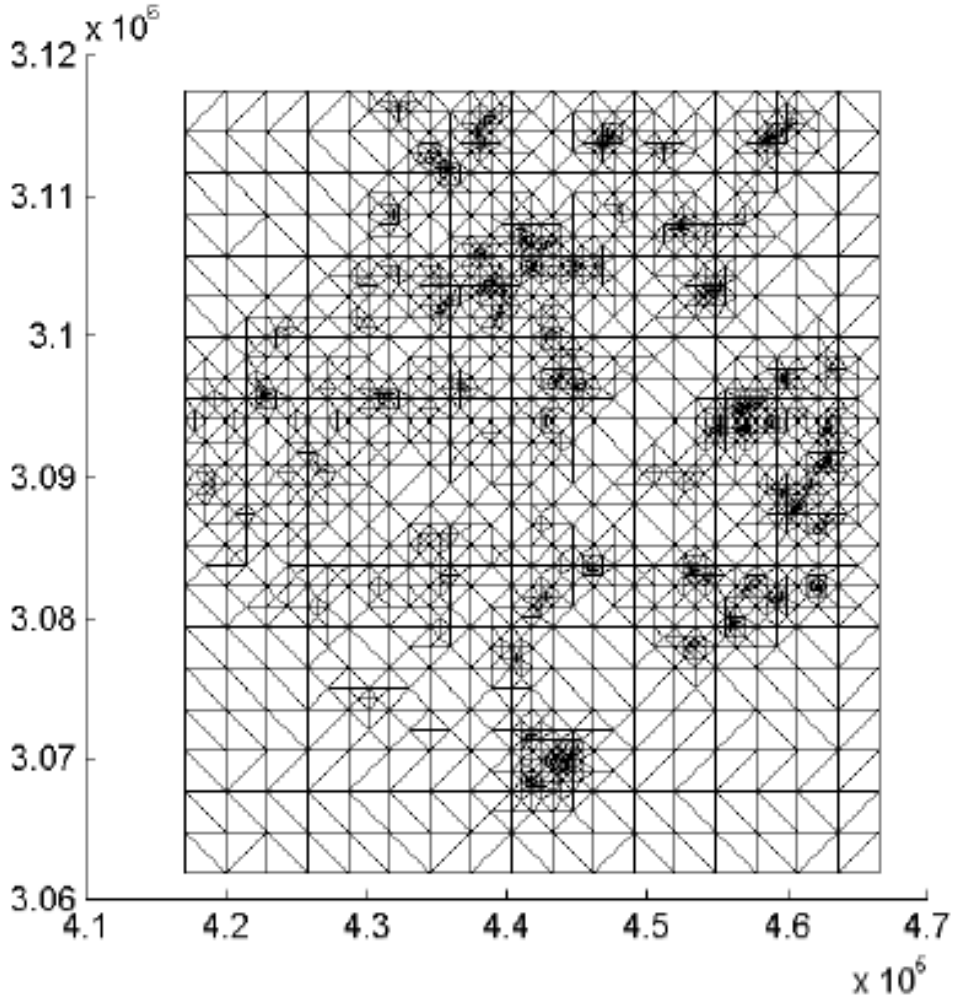

Coarse Mesh
2164 nodes
4247 triangles

Triangular mesh adapted to topography and albedo

Solar radiation modeling
Numerical experiments

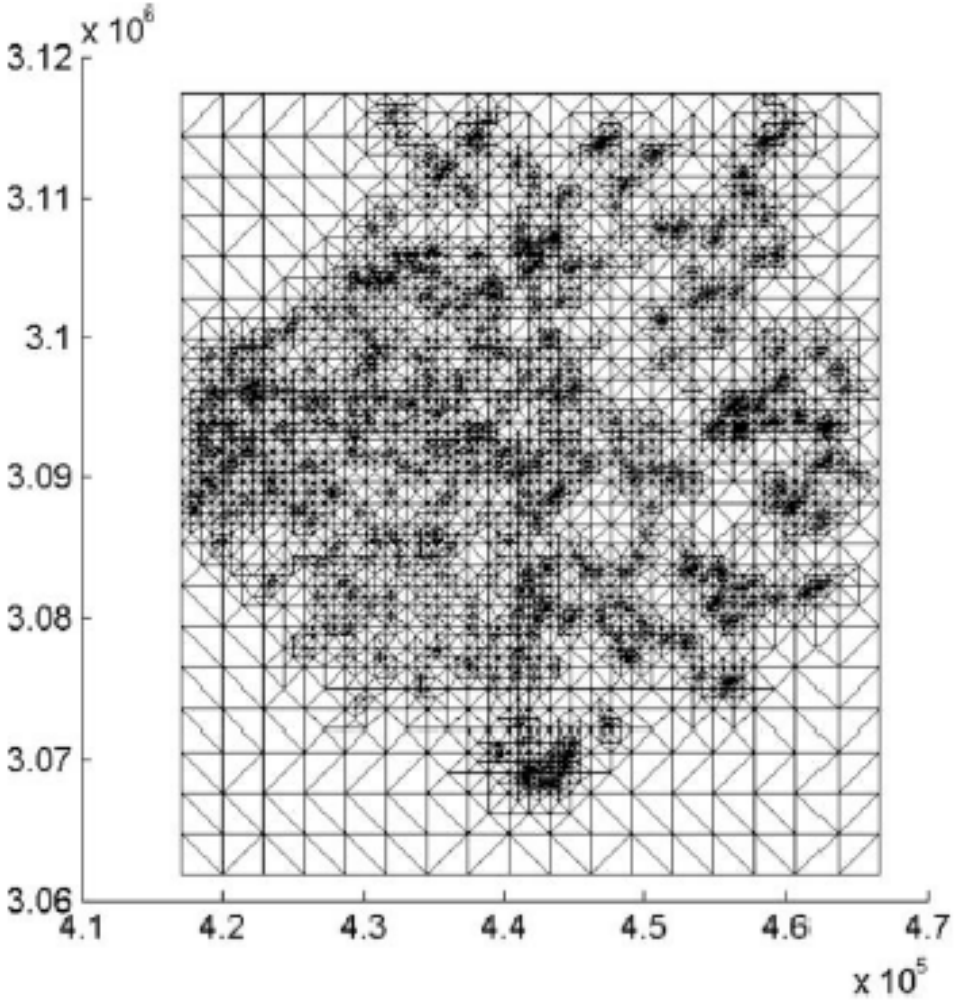

Intermediate mesh
5866 nodes
11683 triangles

Triangular mesh adapted to topography and albedo

Solar radiation modeling
Numerical experiments

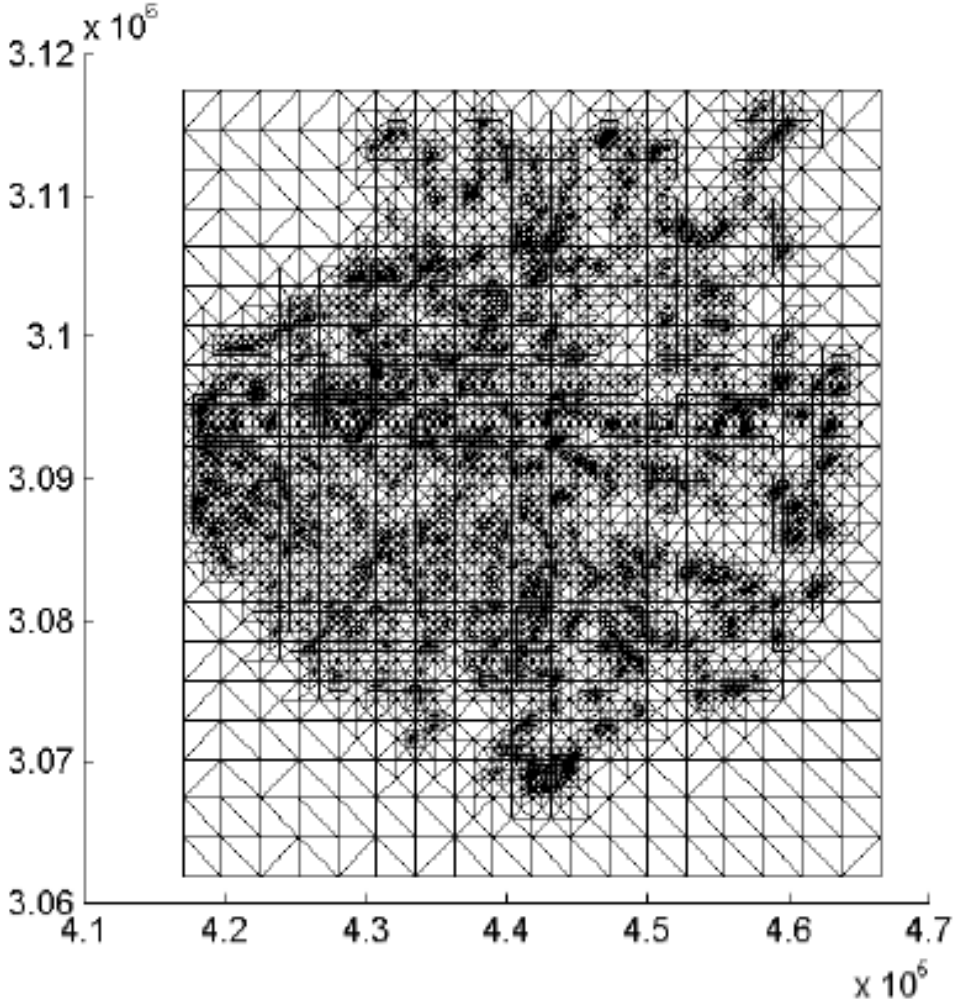

Fine mesh
9276 nodes
18462 triangles

Triangular mesh adapted to topography and albedo

Solar radiation modeling
Numerical experiments

SIANI

Effect of shadows and discretization

Table 4
Average and maximum beam, diffuse, reflected clear-sky radiations in December 2006 after different strategies of shadowing and meshing. Also clear-sky and real-sky global radiations are included. All of them are represented in MJ/m^2.

Strategy	Clear-sky								Real-sky	
	Beam rad.		Diffuse rad.		Reflected rad.		Global rad.		Global rad.	
	Aver.	Max.	Aver.	Max.	Aver.	Max.	Aver.	Max.	Aver.	Max.
No shadow detection	387.90	754.32	76.79	120.36	2.01	24.01	466.71	891.51	322.71	614.04
Regular mesh	389.47	658.99	78.28	108.27	0.61	12.75	468.36	771.91	329.99	551.25
Coarse mesh	382.47	680.57	77.41	108.84	0.87	17.62	460.75	797.75	320.62	536.08
Intermediate mesh	369.54	719.85	76.85	117.30	1.83	21.37	448.22	843.41	314.70	586.25
Fine mesh	362.65	725.40	76.56	115.10	2.29	26.09	441.50	849.78	312.82	601.23

Overestimation of beam radiation with respect to the finer mesh

No shadow detection:	7.0%	(5866 nodes)
Regular mesh:	7.4%	(5913 nodes)
Coarse mesh:	5.5%	(2164 nodes)
Intermediate mesh:	1.9%	(5866 nodes)
Fine mesh:	0.0%	(9276 nodes)

Solar radiation modeling
Predictive approach

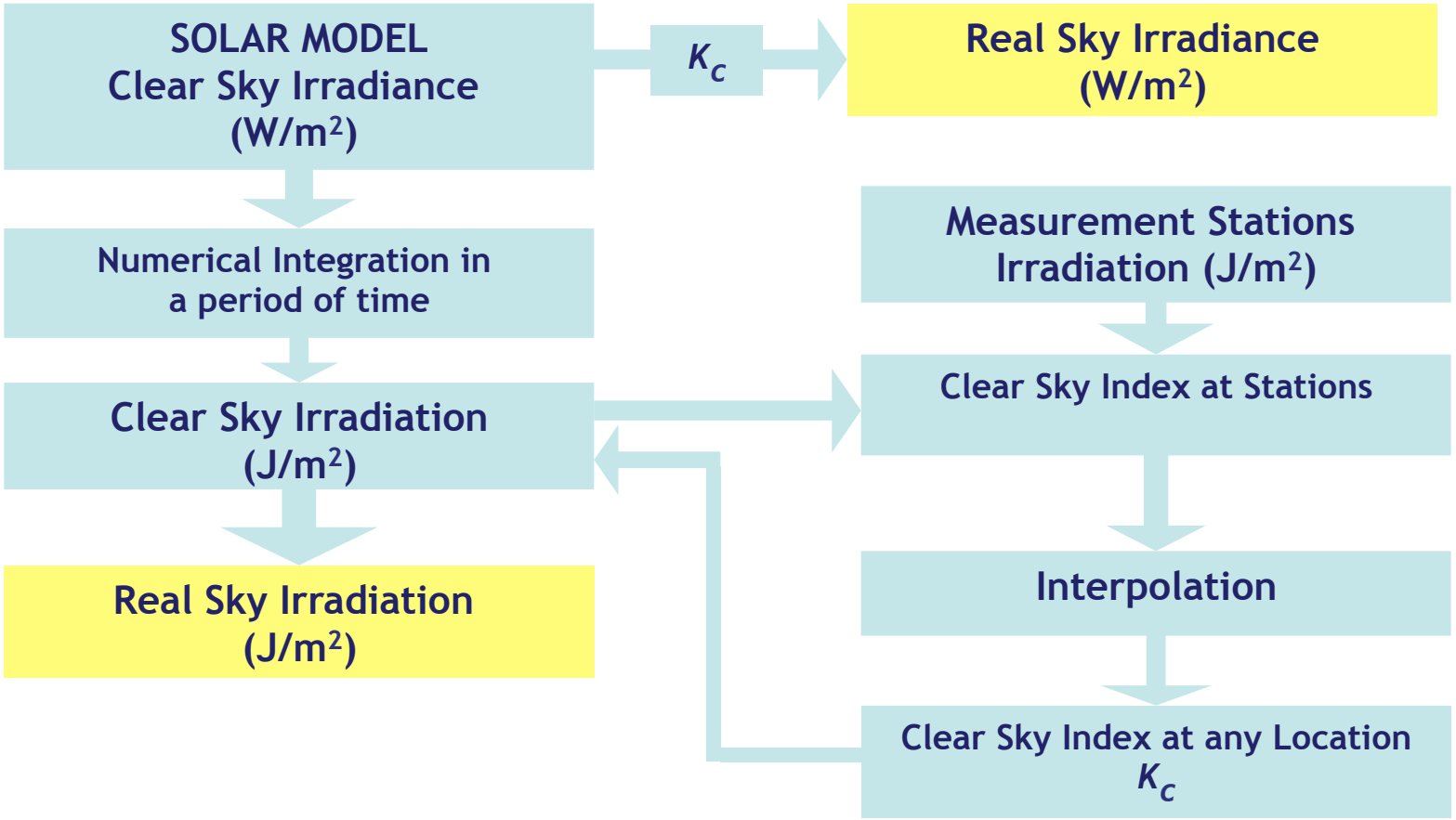

Solar radiation modeling
Predictive approach

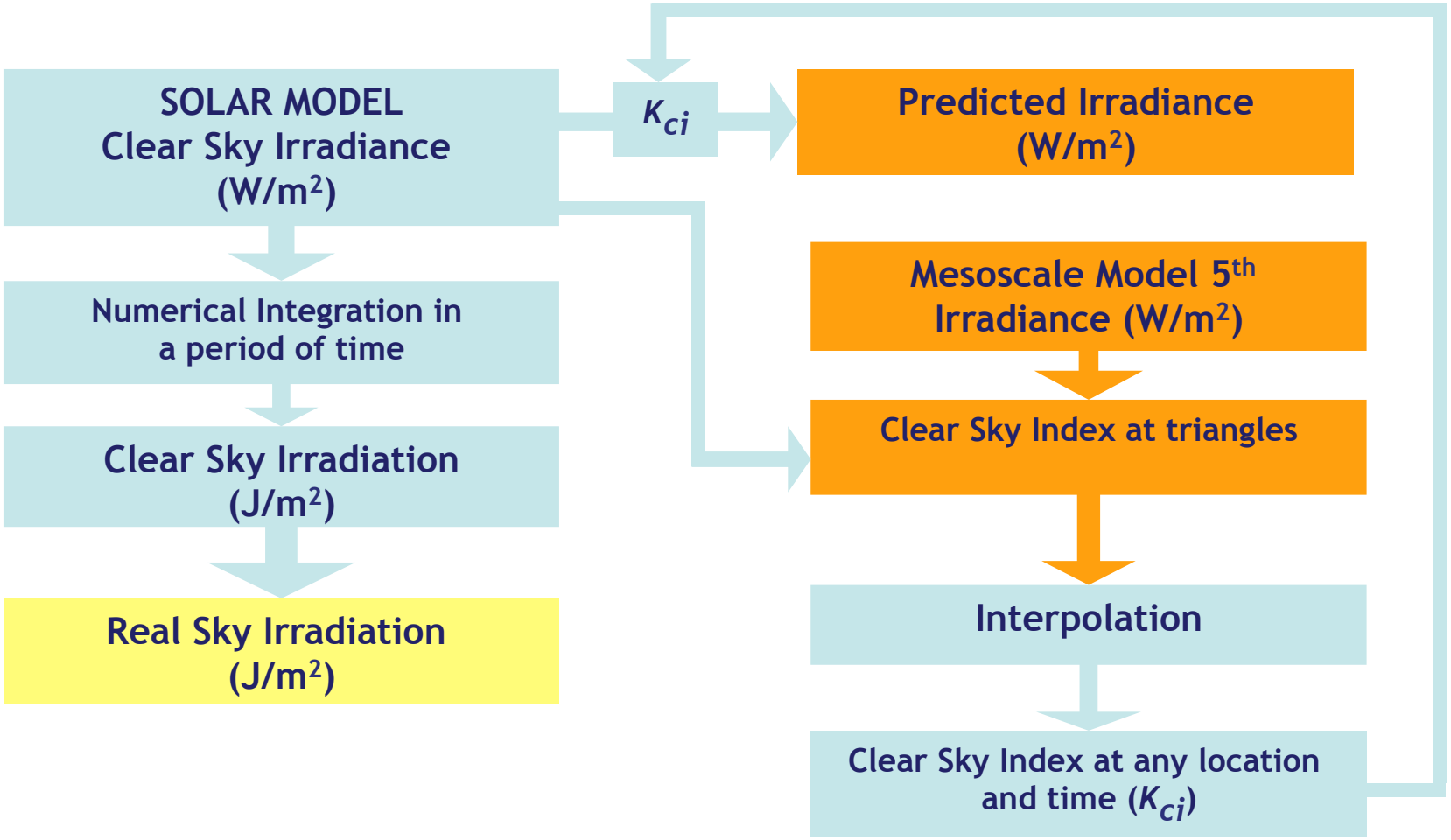

Conclusions

- The adaptive triangulation related to the topography and albedo is essential in order to obtain accurate results of shadow distribution and solar radiation
- Adaptive meshes lead to a minimum computational cost
- Better local predictions, by downscaling results from meteorological forecasting methods

Future research

- Improve the interpolation procedure of clear sky index
- Fully parallelization of the simulation
- Determinate the shadow boundary using ref/deref and mesh adaption by moving nodes

Thank you for your attention

References

[1] F. Díaz, H. Montero, D. Santana, G. Montero, E. Rodríguez, L. Mazorra Aguiar, and A. Oliver. Improving shadows detection for solar radiation numerical models. *Applied Mathematics and Computation*, pages 71–85, 2017.

[2] F. Díaz, G. Montero, J.M. Escobar, E. Rodríguez, and R. Montenegro. An adaptive solar radiation numerical model. *Journal of Computational and Applied Mathematics*, 236(18):4611–4622, Dec 2012.

[3] G. Montero, J.M. Escobar, E. Rodríguez, and R. Montenegro. Solar radiation and shadow modelling with adaptive triangular meshes. *Solar Energy*, 83(7):998–1012, Jul 2009.

[4] Richard Pérez, editor. *Wind Field and Solar Radiation Characterization and Forecasting*. Green Energy and Technology. Springer International Publishing, 2018.